

# Role of Eddy Conductivity in Thermal Transport

W. H. CORCORAN and B. H. SAGE

California Institute of Technology, Pasadena, California

Interest in the course of chemical reactions in turbulent flow has made desirable detailed knowledge of the temperature distribution in flowing streams. One method of predicting the temperature distribution under a variety of conditions is reviewed here, the approach being limited to conditions of local uniform transport of momentum. A discussion of some of the aspects of eddy conductivity is included along with a brief review of the velocity distribution in uniform flow.

The results serve to illustrate the relation of microscopic conditions of flow to the temperature distribution in a turbulently flowing stream. The importance of the molecular Prandtl number upon the transfer process is stressed.

Turbulence exerts a marked influence upon the transport of energy through a fluid as a result of a temperature gradient. The early concepts of a boundary layer in which all the resistance to flow was localized at the edge of the stream appear to be a useful tool in many situations but do not afford a detailed knowledge of the effect of time and position on temperature in various flow processes. The statistical theory of turbulence has made much progress in recent years. The basic contributions of Von Kármán and Howarth (14) and the recent review by Batchelor (2) laid a reasonable theoretical basis for the statistical theory of turbulence. The work of Corrsin (4, 5, 6) at Johns Hopkins is an illustration of the results obtained from the combined action of analysis and experiment. Until the statistical theory of turbulence has reached a somewhat more advanced state than at present, it appears desirable to employ time averages to describe the characteristics of the turbulent-exchange process.

Little experimental information is available concerning the decay of turbulence except in the wake of grids (7). For this reason the present discussion will be limited to steady, uniform flow. Progress is being made by Taylor (25), Uberoi (26), and others in predicting the deviations from isotropy which result from contraction or expansion of flow. The period required for the attainment of steady state in regard to the turbulent-exchange process is also under limited study. For the time being it appears reasonable to limit quantitative considerations to the isotropic characteristics of turbulence, although it must be realized that near boundaries (16) and in streams

which have not yet reached steady state in the Lagrangian sense, marked deviations from isotropy result.

## VELOCITY DISTRIBUTIONS

As noted, the transport of energy in a fluid stream is markedly affected by turbulence. To understand the transport problem it is first necessary to assess the

nature of the momentum transport problem, by examining the velocity distributions in turbulent streams.

It is convenient to employ distance and velocity parameters to describe the velocity distribution near the boundary of a stream (1). These are defined by

$$y^+ = \frac{y_d}{\nu} \sqrt{\frac{\tau_0 g}{\sigma}} = \frac{y_d u_*}{\nu} \quad (1)$$

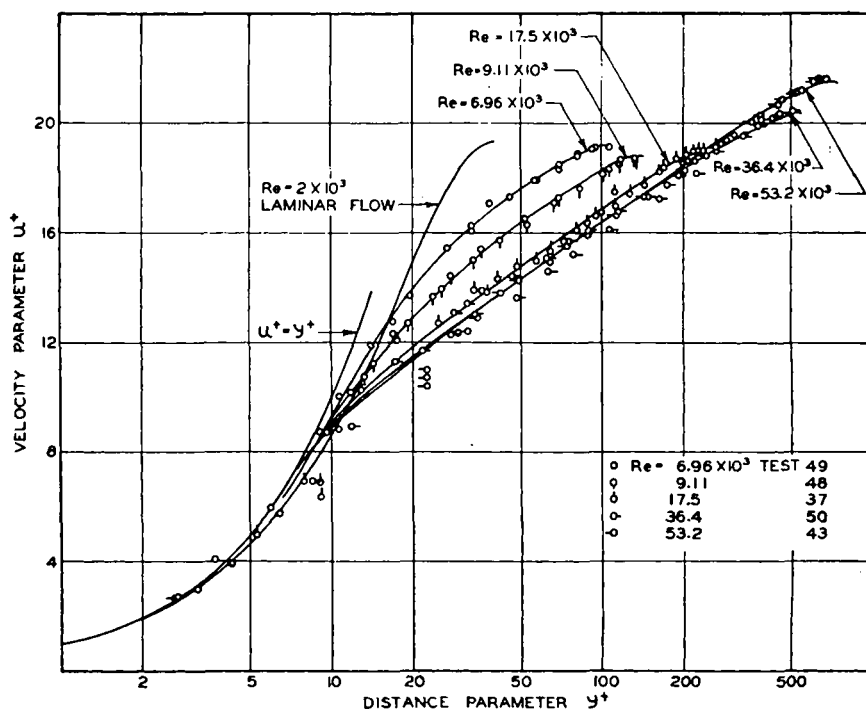


Fig. 1. Experimentally measured velocity distribution.

$$u^+ = \frac{u}{\sqrt{\frac{\tau_0 g}{\sigma}}} = \frac{u}{u_*} \quad (2)$$

These quantities are known as the distance parameter and the velocity parameter,  $y^+$  and  $u^+$  respectively. Experimental measurements (23) of the velocity distribution in an air stream flowing between parallel plates are shown in Figure 1. The experimental results for Reynolds numbers below 20,000 do not agree with the simple theory that  $u^+$  is a single-valued function of  $y^+$  (1). The marked effect of shear upon the behavior in the laminar region is shown for a Reynolds number of 2,000 (23). A comparison of these experimental data with earlier measurements by Laufer (15), Skinner (24), Nikuradse (18), and Deissler (8) is shown in Figure 2. The smoothed data (23) for flow between parallel plates are compared in Figure 3 with Deissler's experimental measurements (8) for flow in a circular conduit. Good agreement is obtained at the higher Reynolds numbers but significant deviation from a single-valued relationship for the flow between parallel plates was found at the lower Reynolds numbers (21). Similar behavior was found in regard to the velocity deficiency (1, 12), as is shown in Figure 4. The velocity deficiency is defined by

$$u_d = \frac{u_m - u}{u_*} = \frac{u_m - u}{\sqrt{\frac{\tau_0 g}{\sigma}}} \quad (3)$$

These data serve to illustrate the complexity of the microscopic velocity distribution in turbulent flow. At the present state of knowledge it appears that for Reynolds numbers below 20,000 the simple generalization of  $u^+$  as a single-valued function of  $y^+$  should not be employed.

For the higher Reynolds numbers this generalization appears to be satisfactory. Utilizing the data of Skinner and Laufer for flow between parallel plates and of Nikuradse and Deissler for flow in a circular conduit gives the relationship of  $u^+$  to  $y^+$  as approximately

$$u^+ = \frac{1}{\sqrt{K_1}} \tanh \sqrt{K_1} y^+ \\ = \frac{1}{0.0695} \tanh 0.0695 \frac{y_d \sqrt{\frac{\tau_0 g}{\sigma}}}{\nu} \\ y^+ < 26.7 \quad (4)$$

$$u^+ = A + \frac{1}{B} \ln y^+ \\ = 5.5 + \frac{1}{0.4} \ln \frac{y_d \sqrt{\frac{\tau_0 g}{\sigma}}}{\nu} \\ y^+ > 26.7 \quad (5)$$

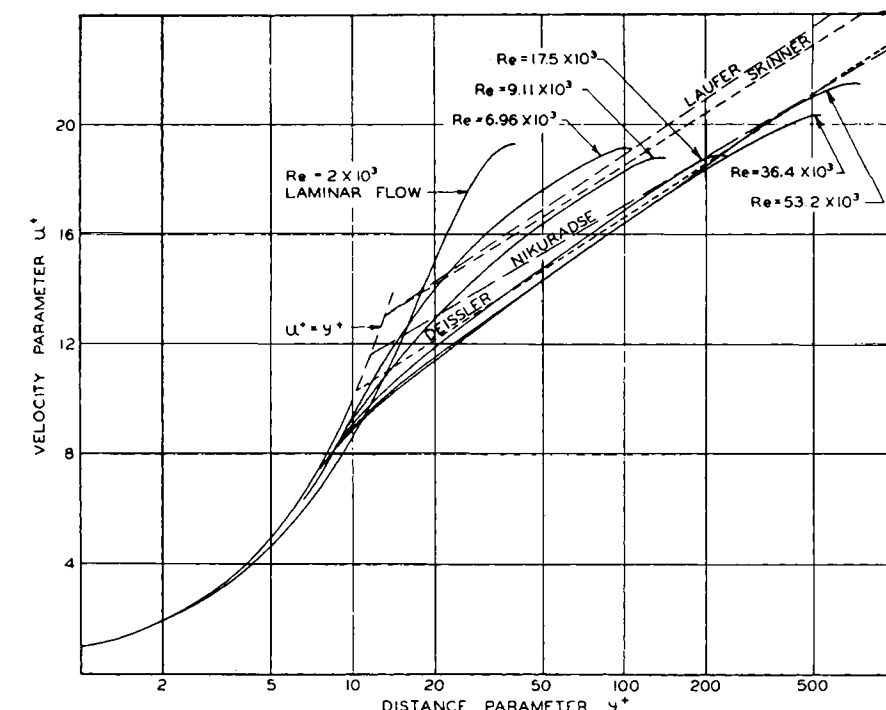


Fig. 2. Comparison of results from different investigators.

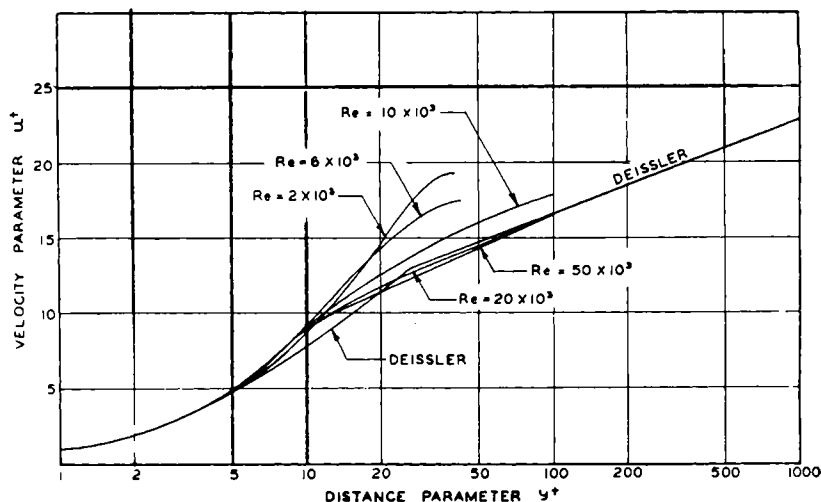


Fig. 3. Comparison of results with flow in circular conduits.

where the fluid properties are constant throughout the stream. These expressions for the flow near the wall (10) and in the main body of the stream (8) yield a continuous first derivative of the velocity with respect to position. However, Equations (4) and (5) assume that  $u^+$  is a single-valued function of  $y^+$ , and, as indicated in the preceding figure, such behavior is encountered only for Reynolds numbers above 20,000 (23). A similar

situation was found in the relation of the velocity deficiency to position.

Deissler (8) prepared an analysis of the relationship of the distance and velocity parameters based upon the similarity hypothesis and certain dimensional considerations as to the factors influencing eddy viscosity. If the shear is assumed constant along with the properties of the fluid, there results for the region near the wall the following expression:

$$y^+ = \frac{1}{n} \frac{\frac{1}{\sqrt{2\pi}} \int_0^{nu^+} e^{-(nu^+)^2/2} d(nu^+)}{\frac{1}{\sqrt{2\pi}} e^{-(nu^+)^2/2}} \quad (6)$$

Fig. 4. Smoothed values of velocity deficiency.

In Equation (6) the quantity  $1/\sqrt{2\pi} e^{-(nu^+)^2/2}$  is the normal error function of  $nu^+$ . Likewise Deissler, following the methods proposed by Von Kármán, obtained an expression of the following form for the variation in  $u^+$  with  $y^+$  in the main body of the stream:

$$\begin{aligned} u^+ &= \frac{1}{K_2} \ln y^+ + C \\ &= \frac{1}{0.36} \ln y^+ + 3.8 \end{aligned} \quad (7)$$

Fig. 5. Comparison of several predictions of velocity distribution.

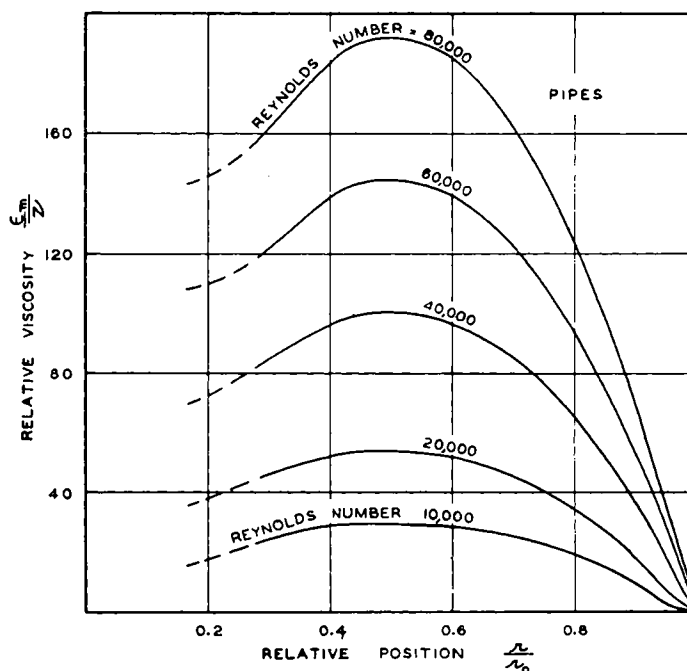
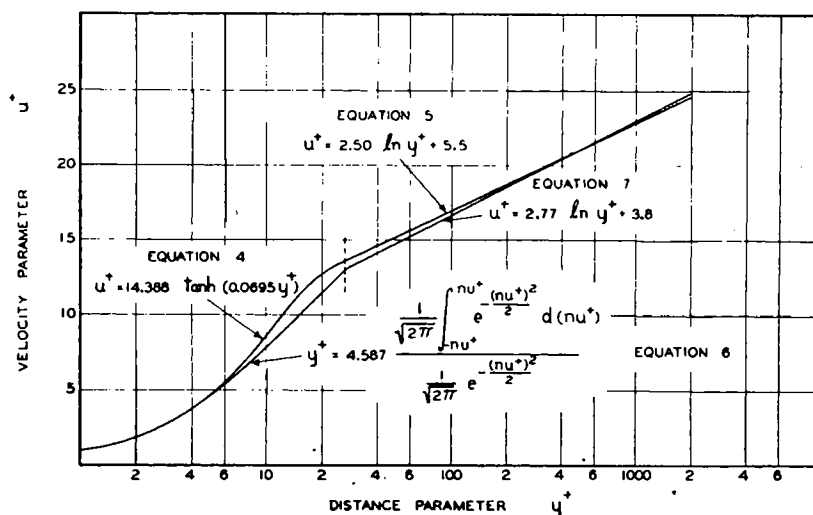
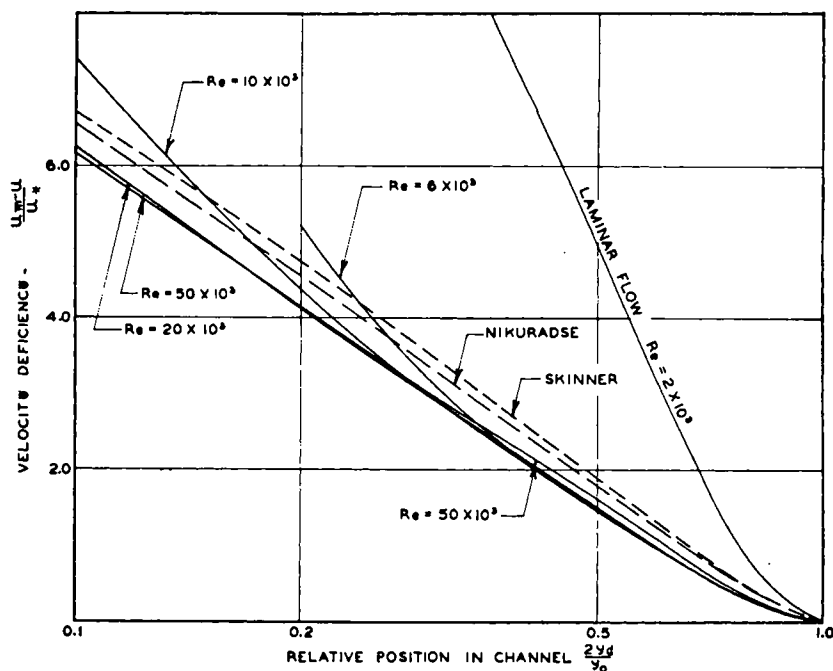
Equation (7) assumes constant shear and fluid properties in the main body of the stream. Figure 5 includes the relations of  $u^+$  and  $y^+$  as described by Equations (4) to (7) inclusive. It is apparent that there is little to choose between the two approaches. In the present discussion most of the comparisons of velocity distribution and of the evaluations of the eddy viscosity have been made on the basis of Equations (4) and (5).

More recently Deissler (9) considered a somewhat different approach and for constant fluid properties suggested the following integral form for the behavior in the boundary layer:

$$u^+ = \int_0^{y^+} \frac{dy^+}{1 + n^2 u^+ y^+ (1 - e^{-n^2 u^+ y^+})} \quad (8)$$

Fig. 6. Relative viscosity as a function of position in flow channel.

In a similar fashion an extension of his more recent approach (9) yielded an expression similar to Equation (5) for the turbulent core. In addition, he extended his treatment of velocity distributions to include the behavior when there is a variation in viscosity with temperature. If all the other properties are considered to be invariant, he suggests the following expressions for the velocity parameter and a temperature parameter:



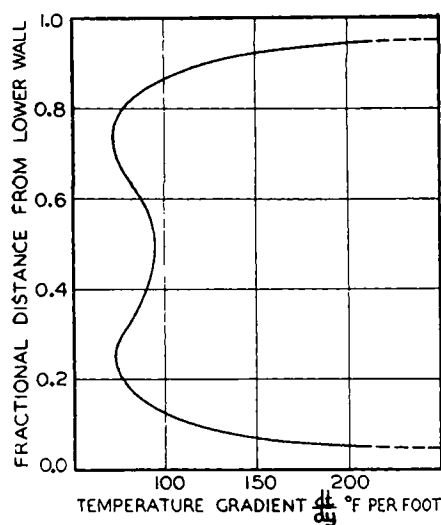


Fig. 7. Temperature gradients for steady uniform flow between parallel plates (upper wall at 105°F. and lower wall at 95°F.).

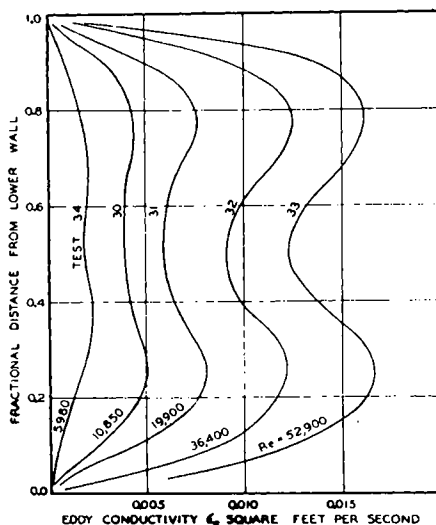


Fig. 8. Influence of Reynolds number upon eddy conductivity.

$$u^+ = \int_0^{y^+} \frac{dy^+}{(1 - \beta t^+)^d + n^2 u^+ y^+ (1 - e^{-(n^2 u^+ y^+) / (1 - \beta t^+)^d})} \quad (9)$$

$$t^+ = \int_0^{y^+} \frac{dy^+}{\frac{1}{Pr_0} + n^2 u^+ y^+ (1 - e^{-(n^2 u^+ y^+) / (1 - \beta t^+)^d})} \quad (10)$$

In the application of Equations (9) and (10) it was assumed by Deissler (9) that the variation in viscosity could be described by

$$\frac{\mu}{\mu_0} = (1 - \beta t^+)^d \quad (11)$$

The simplification of Equation (9) to the form of Equation (8) when the viscosity is independent of position is evident. Deissler (8, 9) discussed the underlying assumptions and boundary conditions involved in the foregoing equations. In the interest of brevity these matters have not been discussed in detail.

It should be realized that the preceding equations are applicable only for the higher Reynolds numbers and that significant errors may be introduced if they are employed for Reynolds numbers below about 20,000. In the following discussion it will be assumed that the relationships of  $u^+$  and  $y^+$  established experimentally as shown in Figures 1 and 2 apply at Reynolds numbers below 20,000 and as indicated in Equations (4) and (5) at higher Reynolds numbers.

The velocity-position data may be used in computing the eddy viscosity which has application in relating momentum transfer with heat and mass transfer. Von Kármán (13) defined an eddy viscosity for steady, uniform flow between parallel plates as

$$\epsilon_m = \frac{g\tau}{\sigma \frac{du}{dy}} - \nu = \frac{g}{2\sigma} \frac{\partial P}{\partial x} \frac{\partial y}{\partial (y^2)} - \nu \quad (12)$$

It is convenient to consider the total viscosity as defined by

$$\epsilon_m = \epsilon_m + \nu \quad (13)$$

The relative viscosity  $\epsilon_m/\nu$  may be calculated from the velocity distribution, pressure drop, and fluid properties.

At Reynolds numbers above 20,000 expressions which are based on the generalization shown in Equation (4) may be developed (22) for evaluation of the relative viscosity. At values of  $y^+$  less than 26.7 there results

$$\frac{\epsilon_m}{\nu} = \frac{l}{l_0} \cosh^2 \left[ 0.0695 \left( \frac{l_0 - l}{\nu} \right) \sqrt{\frac{\tau_0 g}{\sigma}} \right] \quad (14)$$

or

$$\frac{\epsilon_m}{\nu} = \frac{l}{l_0} \cosh^2 \left[ 0.0695 \left( \frac{l_0 - l}{\nu} \right) U \sqrt{\frac{f}{2}} \right] \quad (15)$$

For larger values of  $y^+$  the relative viscosity is obtained by use of Equation (5):

$$\frac{\epsilon_m}{\nu} = \frac{0.4}{\nu} \sqrt{\frac{\tau_0 g}{\sigma}} \left( \frac{l}{l_0} \right) (l_0 - l) \quad (16)$$

or

$$\frac{\epsilon_m}{\nu} = 0.4 \frac{U}{\nu} \sqrt{\frac{f}{2}} \left( \frac{l}{l_0} \right) (l_0 - l) \quad (17)$$

Deissler (9) also developed an expression for the relative viscosity near the wall of the conduit when considering constant physical properties of the fluid

$$\frac{\epsilon_m}{\nu} = \frac{\epsilon_m}{\mu_0} = n^2 u^+ y^+ (1 - e^{-n^2 u^+ y^+}) \quad (18)$$

If variation only in molecular viscosity is considered, the last term of Equation (18) becomes  $e^{-n^2 u^+ y^+ / (\mu/\mu_0)}$  where  $\mu/\mu_0$  may be obtained by development of Equation (11).

The relative viscosity (23) in a circular conduit which is large in comparison with the thickness of the boundary layer is presented in Figure 6 for constant physical properties. It is apparent that both the Reynolds number and the position in the steady, uniform stream exert a pronounced influence upon the relative eddy viscosity. Again it is emphasized that for a Reynolds number below 20,000 the relative viscosity is subject to uncertainty as a result of the difficulty in predicting the velocity distribution with accuracy.

### EDDY CONDUCTIVITY

After estimating values of the eddy viscosity, it is possible by making reasonable assumptions to use these data in establishing values of the analogous term for thermal transport, the eddy conductivity (13). Before such relations are considered, however, it is desirable first to consider the nature of the eddy conductivity. It has been defined in the following way:

$$\begin{aligned} \epsilon_c &= -\frac{\dot{Q}}{C_p \sigma} \frac{dy}{dt} - K \\ &= -\frac{\dot{Q}}{C_p \sigma} \frac{dy}{dt} - \frac{k}{C_p \sigma} \end{aligned} \quad (19)$$

Likewise, the total conductivity may be described as

$$\epsilon_c = \epsilon_c + K = -\frac{\dot{Q}}{C_p \sigma} \frac{dy}{dt} \quad (20)$$

Under steady, uniform conditions all the variables in Equations (19) and (20) may be measured directly. For example, the temperature gradient normal to the flow of air between parallel plates at a mean temperature of 100°F. is shown in Figure 7 for a gross velocity of 28.1 ft./sec. and a Reynolds number of 17,100. The average temperature gradient was 164.5°F./ft. Thermal flux may be readily measured under steady conditions by conventional calorimetric techniques. From such information it is possible to establish the eddy conductivity as a function of position in the stream and the Reynolds number by use of Equation (19). The results of these measurements (19, 20) for the flow of air between parallel plates are shown in Figure 8.

In the treatment of the relation between momentum transfer and heat transfer, the Prandtl number is often used as a means of correlating data. It is convenient to define three Prandtl numbers, one

relating to molecular transport, one to eddy transport, and one to the total transport. These are shown, respectively, in the following expressions:

$$Pr_m = \frac{\nu}{K} \quad (21)$$

$$Pr_e = \frac{\epsilon_m}{\epsilon_c} \quad (22)$$

$$Pr = \frac{\epsilon_m}{\epsilon_c} = \frac{\epsilon_m + \nu}{\epsilon_c + K} \quad (23)$$

The effect of Reynolds number and position in the stream upon the total and

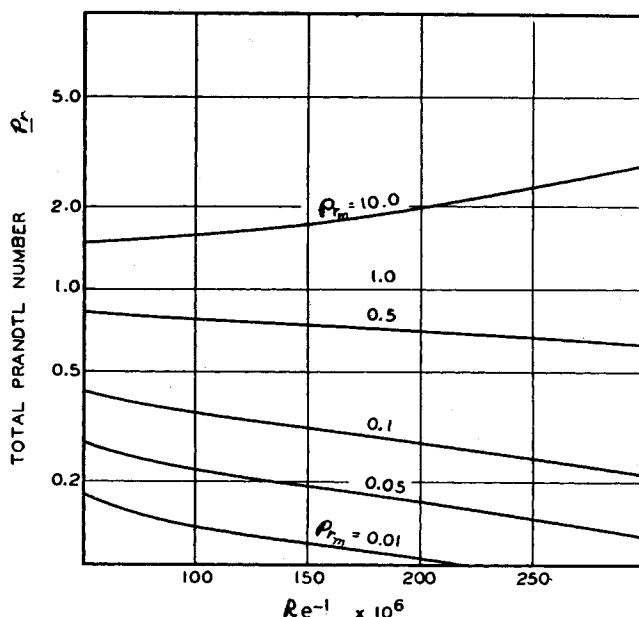


Fig. 9. Estimated effect of Reynolds number and molecular Prandtl number on total Prandtl number in turbulent core.

eddy Prandtl numbers was investigated for a stream of air (20). It was found in this case that the Prandtl numbers did not vary rapidly with position near the center of the stream and that for an increase in the Reynolds number the eddy Prandtl number gradually increased. More recent unpublished data for air under a slightly different level of turbulence, however, indicate the reverse trend at Reynolds numbers above 20,000. Rather complicated trends in the turbulent Schmidt number are also encountered with variations in conditions of flow. On the basis of the experimental evidence accumulated, it appears that the eddy

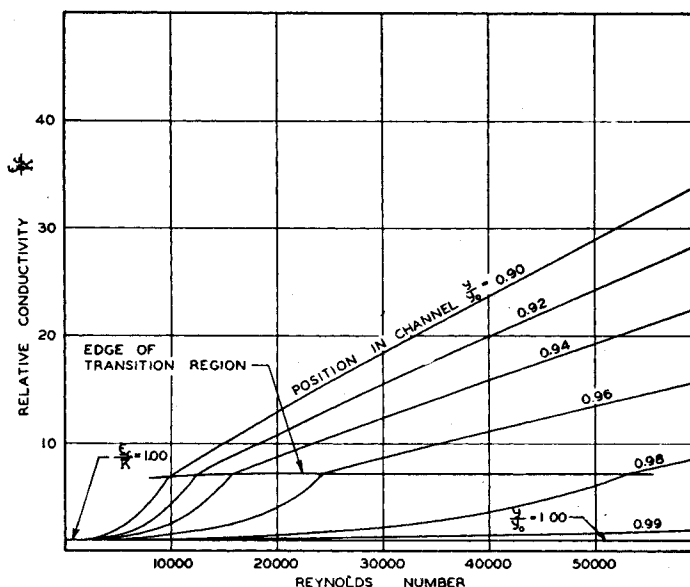


Fig. 10. Ratio of total to molecular conductivity on basis of Reynolds analogy.

Prandtl number for air is sensitive to the conditions of flow beyond those described by the gross Reynolds number. The primary uncertainty may well lie in the eddy viscosity, which is most sensitive to momentum transport.

The total Prandtl number is estimated to be a marked function of the Reynolds number (20) and the molecular Prandtl number, as shown in Figure 9. The trends as to the effect of the molecular Prandtl number shown here are based in a large measure upon theoretical considerations (11) and are subject to uncertainties.

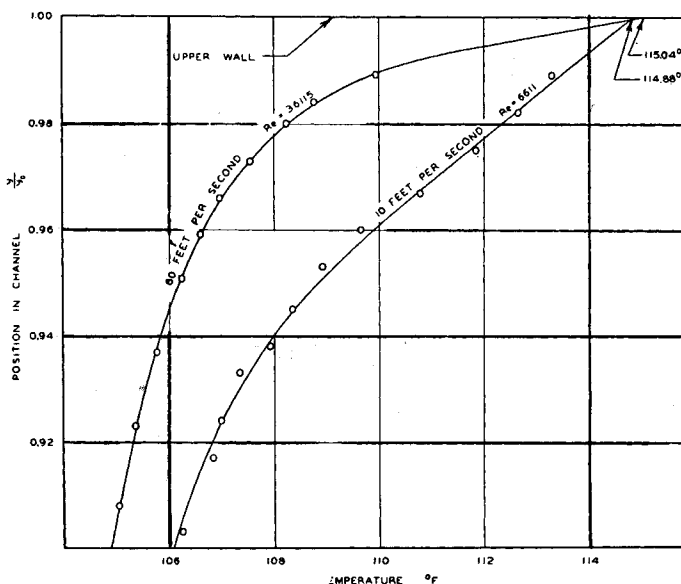


Fig. 11. Temperature distribution near wall.

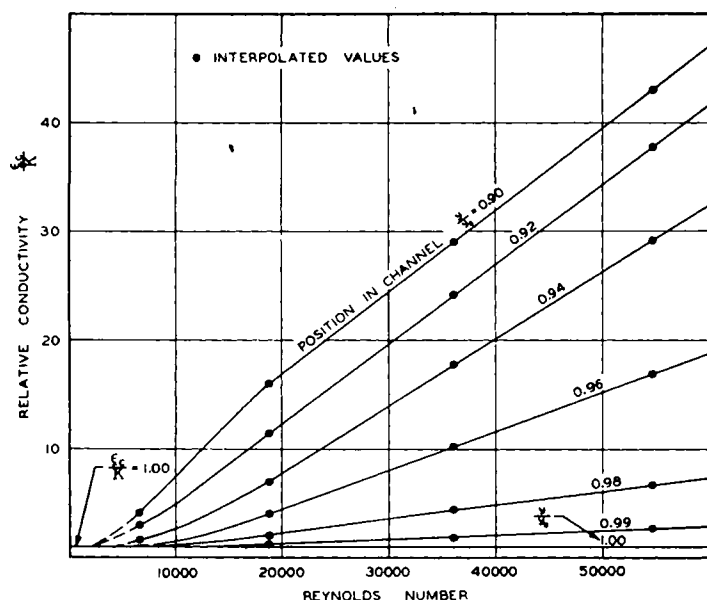
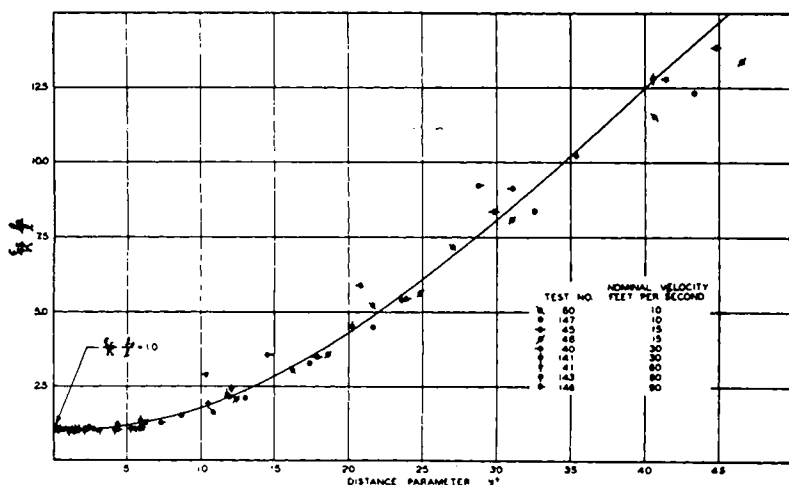


Fig. 12. Effect of Reynolds number upon relative conductivity.

#### BEHAVIOR IN THE BOUNDARY LAYER

It is obvious from the variations of the eddy conductivity with position that the greater part of the resistance to thermal transport is located near the boundary of the stream. From the characteristic transport of momentum in the boundary layer, which is presented in the first part of this discussion, the relative conductivity may be evaluated as a function of position and Reynolds number for that region, as shown in Figure 10. This figure assumes that the eddy conductivity and eddy viscosity are equal, which has been found not to be strictly true (20). However, the complex nature of turbulence near the boundary layer and the indication of marked deviations from isotropic behavior in this region introduce added uncertainties. For this reason it does not appear worth while to refine the information presented in Figure 10 by taking into account the deviations from Reynolds analogy (20). There is a marked effect of position in the



channel on the relation between Reynolds number and the relative conductivity  $\epsilon_c/K$  in steady, uniform flow.

The temperature variation ( $\beta$ ) near the wall associated with the flow of air between parallel plates is shown in Figure 11. A marked effect of Reynolds number upon temperature distribution is evident. The relative conductivity based upon these experimental data ( $\beta$ ) is shown in Figure 12 as a function of Reynolds number.

The total conductivity obtained experimentally is compared with the experimental and calculated total viscosities in Figure 13. It can be seen that there is a marked similarity between the curves for eddy conductivity and eddy viscosity. Because of the thicker boundary layer the curve for the calculated total viscosity at the lower Reynolds number does not show the discontinuity in slope as evi-

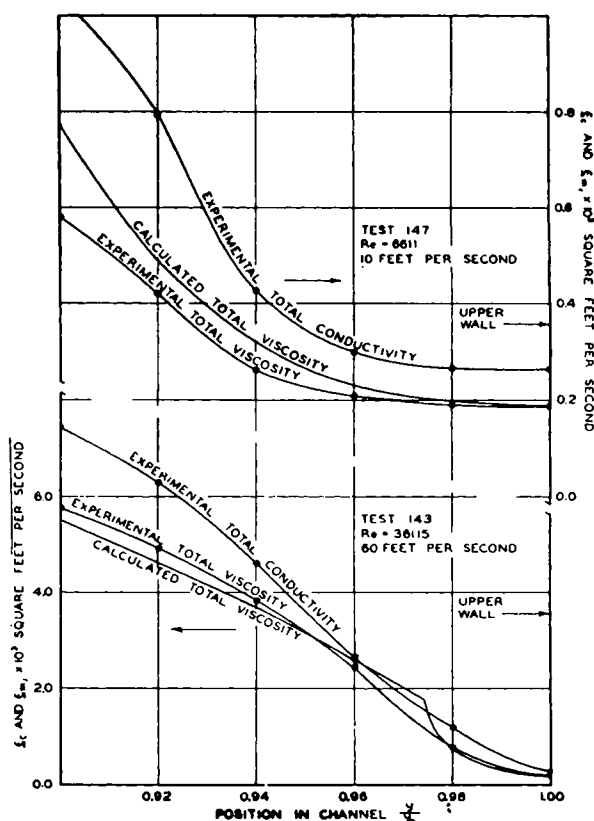


Fig. 13. Comparison of total conductivity and total viscosity.

denced in the curve at the higher Reynolds number.

It is of interest to compare the variation of the relative conductivity as a function of the distance parameter  $y^+$ . Such behavior is shown in Figure 14, where a relative conductivity term is plotted as a function of the distance parameter  $y^+$ .

Fig. 14. Effect of distance parameter upon average relative conductivity.

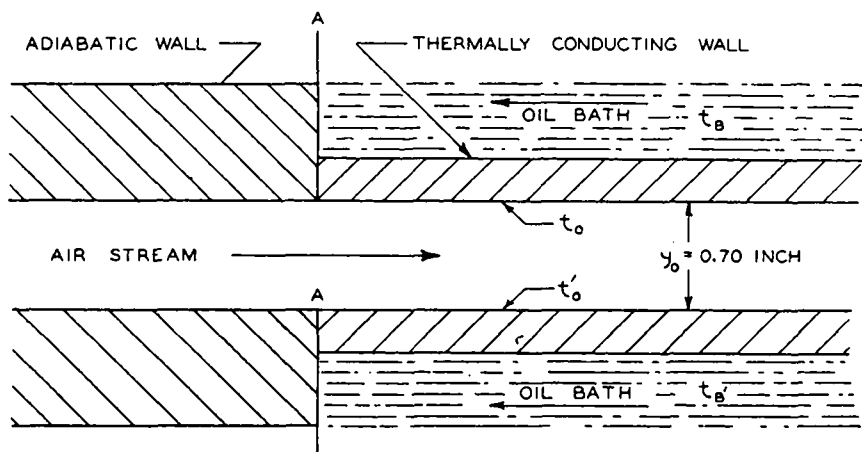


Fig. 15. Schematic diagram of two-dimensional air stream.

#### ESTIMATION OF TEMPERATURE DISTRIBUTION

It is often of interest to predict the temperature distribution in flow which is substantially uniform with regard to the transfer of momentum and non-uniform with respect to thermal transport. Such a situation is portrayed in Figure 15 for two-dimensional, steady, uniform flow between parallel plates. Under the circumstances the over-all energy balance may be expressed as

$$\frac{\partial \epsilon_c}{\partial y} \frac{\partial T}{\partial y} = u_x \frac{\partial T}{\partial x} \quad (24)$$

Equation (24) neglects the effect of changes in elevation, kinetic energy, and pressure upon the characteristics of the stream for both the gross and turbulent motion. This nonlinear equation may be solved by field methods or by an electrical analogue. It does not appear worth while to consider the details of the solution of this partial differential equation except to indicate that the resistance of the thermally conducting wall must be taken into account to establish the boundary conditions for the fluid. By use of the specific characteristics of a copper wall for a two-dimensional channel, the wall-temperature distribution was both calculated and measured as a function of downstream position as shown in Figure 16. It is apparent that the predicted and experimental wall temperatures were in satisfactory agreement. Comparisons of the predicted and calculated temperatures in the stream at several positions downstream for the same channel are shown in Figure 17, where good agreement between the experimental and predicted temperature distributions was obtained. In this instance the air was introduced at 100°F. and the upper and lower walls were at the indicated temperatures. The agreement of the experimentally determined and predicted temperatures with other boundary conditions is shown in Figure 18. In this case the air was introduced at 100°F., which corresponded to the upper wall temperature; whereas the lower wall was at 85°F., as before. Agreement was also obtained for this set of conditions. It is possible to predict the thermal flux at the wall by integration of Equation (24) for specific boundary conditions. Under these circumstances the gross heat-transfer coefficient based upon the bulk temperatures of the stream has been calculated for comparison and is shown in Figure 19. At the transition from the adiabatic to the conducting wall a rapid change in conditions takes place and the actual thermal transfer coefficient is large. However, the coefficient approaches a uniform value at a downstream distance approximately equal to forty times the channel height and is in good agreement with predictions made by methods described by McAdams (17).

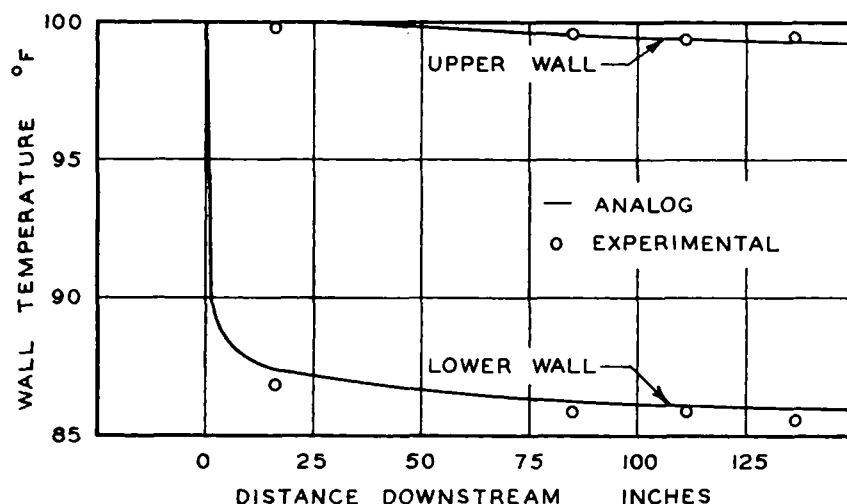
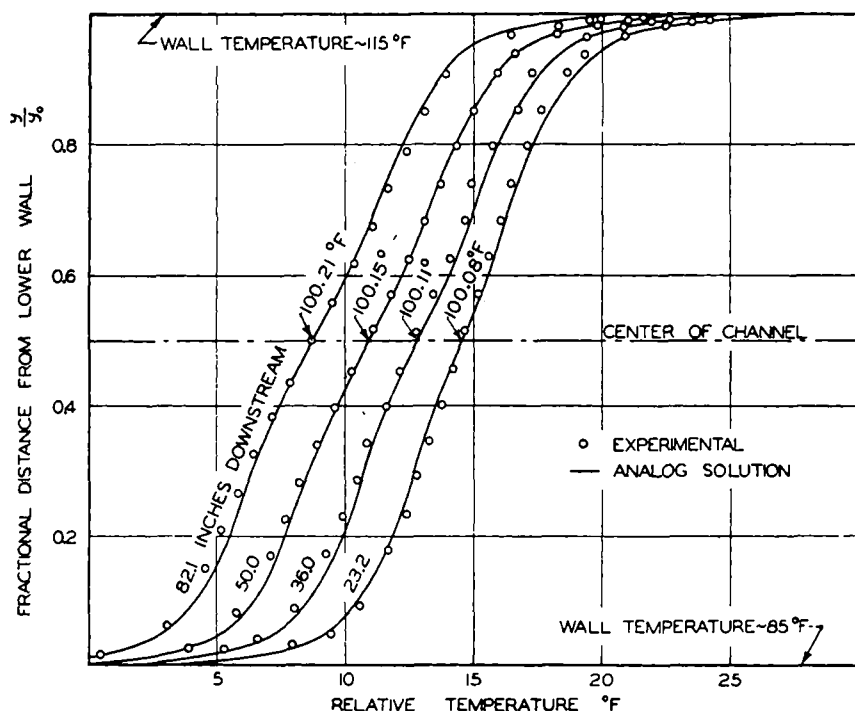


Fig. 16. Variation in wall temperatures with downstream position.



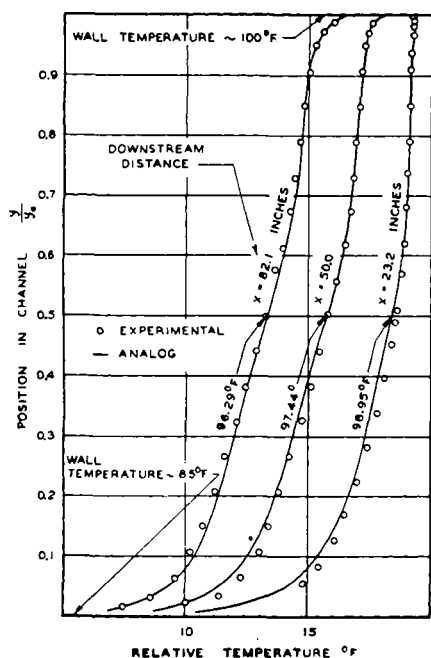


Fig. 18. Temperature distribution in flow channel with upper oil bath temperature at 100° F.

#### ACKNOWLEDGMENT

Figures 1 to 4, 6, 7, and 10 to 18 are reprinted by permission of the copyright owner, *Industrial and Engineering Chemistry*. Figure 19 is reprinted by permission of the copyright owner, Institution of Mechanical Engineers, London, England. B. Lawson Miller assisted in the assembly of the manuscript and L. Fay Prescott reviewed the finished copy.

#### NOTATION

$A, B$  = constants  
 $C$  = constant of integration  
 $C_p$  = isobaric heat capacity, ft./°F.  
 $d$  = differential operator  
 $e$  = base of natural logarithms  
 $f$  = friction factor  
 $g$  = acceleration due to gravity, ft./sec.<sup>2</sup>  
 $K_1, K_2$  = constants of proportionality  
 $k$  = thermal conductivity, ft./(sec.) (ft.) (°F.)  
 $l$  = distance from center of channel, ft.  
 $l_0$  = distance from center of channel to wall, ft.  
 $\ln$  = natural logarithm  
 $n$  = constant of proportionality taken as 0.109  
 $P$  = pressure, lb./sq. ft.  
 $Pr$  = total Prandtl number  
 $Pr_r$  = eddy Prandtl number  
 $Pr_m$  = molecular Prandtl number  
 $Pr_0$  = Prandtl number with properties evaluated at  $t_0$   
 $\dot{Q}$  = thermal flux, lb./(ft.) (sec.)  
 $r$  = radius, ft.

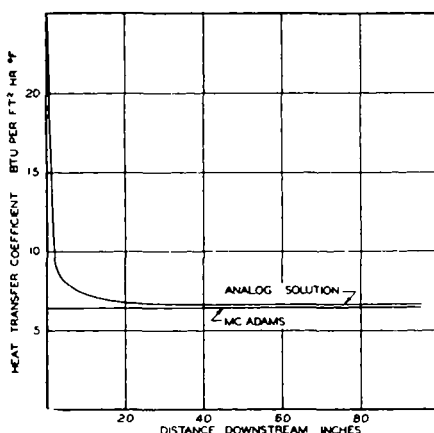


Fig. 19. Thermal transfer coefficient near entrance to flow channel.

$r_0$  = radius of conduit, ft.  
 $Re$  = Reynolds number  
 $T$  = absolute temperature, °R.  
 $t$  = temperature, °F.  
 $t^+$  = temperature parameter,

$$\frac{(t_0 - t)C_p g \tau_0}{\dot{Q} \sqrt{\frac{\tau_0}{\rho_0}}} = \frac{1 - \frac{t}{t_0}}{\beta}$$

$t_B$  = temperature of bath, °F.  
 $t_0$  = temperature of wall, °F.  
 $U$  = gross velocity, ft./sec.  
 $u$  = point velocity, ft./sec.  
 $u_*$  = friction velocity,  $\sqrt{\tau_0 g / \sigma}$ , ft./sec.  
 $u^+$  = velocity parameter defined by Equation (2)  
 $u_d$  = velocity deficiency defined by Equation (3)  
 $u_m$  = maximum velocity, ft./sec.  
 $u_x$  = velocity in  $x$  direction, ft./sec.  
 $x$  = downstream distance, ft.  
 $y$  = distance from wall, ft.  
 $y^+$  = distance parameter, defined by Equation (1)  
 $y_d$  = distance from nearest wall, ft.  
 $y_0$  = separation of plates, ft.  
 $\beta$  = heat transfer parameter,

$$\frac{\dot{Q} \sqrt{\frac{\tau_0}{\rho_0}}}{C_p g \tau_0 t_0}$$

$\epsilon_e$  = eddy conductivity, sq. ft./sec.  
 $\epsilon_c$  = total conductivity,  $(\epsilon_e + K)$ , sq. ft./sec.  
 $\epsilon_m$  = eddy viscosity, sq. ft./sec.  
 $\epsilon_m$  = total viscosity,  $(\epsilon_m + \nu)$ , sq. ft./sec.  
 $K$  = thermometric conductivity, sq. ft./sec.  
 $\mu$  = absolute viscosity of fluid, (lb.) (sec.)/sq. ft.  
 $\mu_0$  = absolute viscosity of fluid evaluated at  $t_0$ , (lb.) (sec.)/sq. ft.

$\nu$  = kinematic viscosity, sq. ft./sec.  
 $\nu_0$  = kinematic viscosity evaluated at wall, sq. ft./sec.  
 $\rho_0$  = density of fluid evaluated at wall, (lb.) (sec.)/ft.<sup>3</sup>  
 $\sigma$  = specific weight, lb./cu. ft.  
 $\tau$  = shear, lb./sq. ft.  
 $\tau_0$  = shear at wall, lb./sq. ft.  
 $\partial$  = partial differential operator

#### Superscripts

$d$  = viscosity exponent  
 $'$  = lower oil bath

#### LITERATURE CITED

1. Bakhmeteff, B. A., "The Mechanics of Turbulent Flow," Princeton University Press, Princeton (1941).
2. Batchelor, G. K., "The Theory of Homogeneous Turbulence," University Press, Cambridge (1953).
3. Cavers, S. D., N. T. Hsu, W. G. Schlinger, and B. H. Sage, *Ind. Eng. Chem.*, **45**, 2139 (1953).
4. Corssin, S., *J. Aero. Sci.*, **18**, 417 (1951).
5. *Ibid.*, **22**, 469 (1951).
6. ———, *Proc. Third Midwestern Conference on Fluid Mechanics*, p. 435, Univ. Minnesota (1953).
7. Davis, L., *Jet Propulsion Lab. Rept. 3-22*, Pasadena, Calif. (1950).
8. Deissler, R. G., *Natl. Advisory Comm. Aeronaut., Tech. Note 2138* (1950).
9. *Ibid.*, 3145 (1954).
10. Dunn, L. G., W. B. Powell, and H. S. Seifert, paper at Roy. Aeronaut. Soc., Third Anglo-American Aeronaut. Conf. (1951).
11. Jenkins, R., Ph.D. thesis, Calif. Inst. Technol., Pasadena, Calif. (1950).
12. Kármán, von, Th., *J. Aero. Sci.*, **1**, 1 (1934).
13. ———, *Trans. Am. Soc. Mech. Engrs.*, **61**, 705 (1939).
14. ———, and L. Howarth, *Proc. Roy. Soc. (London)*, **A164**, 192 (1938).
15. Laufer, J., *Natl. Advisory Comm. Aeronaut., Tech. Note 2123* (1950).
16. *Ibid.*, 2954 (1953).
17. McAdams, W. H., "Heat Transmission," McGraw-Hill Book Company, Inc., New York (1942).
18. Nikuradse, J., *Forsch. Gebiete Ingenieurw., Forschungsheft 356* (1932).
19. Page, F., Jr., W. H. Corcoran, W. G. Schlinger, and B. H. Sage, *Am. Doc. Inst.*, Washington, D. C., Doc. 3293 (1950).
20. ———, *Ind. Eng. Chem.*, **44**, 419 (1952).
21. Page, F., Jr., W. G. Schlinger, D. K. Breaux, and B. H. Sage, *Am. Doc. Inst.*, Washington, D. C., Doc. 3294 (1951).
22. Schlinger, W. G., V. J. Berry, J. L. Mason, and B. H. Sage, *Ind. Eng. Chem.*, **45**, 662 (1953).
23. Schlinger, W. G., and B. H. Sage, *Ind. Eng. Chem.*, **45**, 2636 (1953).
24. Skinner, G., thesis, California Inst. Technol., Pasadena, Calif. (1950).
25. Taylor, G. I., *Advisory Comm. Aeronaut. (London), Tech. Rept. 2*, 423 (1916-17).
26. Uberoi, M. S., *Natl. Advisory Comm. Aeronaut., Tech. Note 1865* (1949).